

## Epitaxial growth of *M*-type Ba-hexaferrite films on MgO (111)||SiC (0001) with low ferromagnetic resonance linewidths

Zhaohui Chen, Aria Yang, Antone Gieler, V. G. Harris, and C. Vittoria  
*Department of Electrical and Computer Engineering, Northeastern University, Boston, Massachusetts 02115, USA*

P. R. Ohodnicki, K. Y. Goh, and M. E. McHenry  
*Materials Science and Engineering, Carnegie Mellon University, Pittsburgh, Pennsylvania 15213, USA*

Zhuhua Cai, Trevor L. Goodrich, and Katherine S. Ziemer<sup>a)</sup>  
*Chemical Engineering Department, Northeastern University, Boston, Massachusetts 02115, USA*

(Received 21 July 2007; accepted 13 September 2007; published online 31 October 2007)

Barium hexaferrite (BaM) films were deposited on 10 nm MgO (111) films on 6H silicon carbide (0001) substrates by pulsed laser deposition from a homogeneous BaFe<sub>12</sub>O<sub>19</sub> target. The MgO layer, deposited by molecular beam epitaxy, alleviated lattice mismatch and interdiffusion between film and substrate. X-ray diffraction showed strong crystallographic alignment while pole figures exhibited reflections consistent with epitaxial growth. After optimized annealing, these BaM films have a perpendicular magnetic anisotropy field of 16 900 Oe, a magnetization (as  $4\pi M_s$ ) of 4.4 kG, and a ferromagnetic resonance peak-to-peak derivative linewidth at 53 GHz of 96 Oe, thus demonstrating sufficient properties for microwave device applications. © 2007 American Institute of Physics. [DOI: 10.1063/1.2794011]

It has been a longstanding goal of the microwave device community to integrate nonreciprocal microwave devices (e.g., circulators, isolators, phase shifters, etc.) with semiconductor device platforms in order to meet the demands of increasing microwave power and reduced device volume.<sup>1,2</sup> Previous attempts to deposit ferrite materials onto silicon and gallium arsenide failed in that the high temperatures required for the processing of low microwave loss ferrite materials resulted in either alloying with the silicon substrate or chemical disassociation of the GaAs substrate. In both cases, the films' microwave performances degraded. Today, there are new options for high power microwave semiconductor materials, which include the wide bandgap materials silicon carbide (SiC) and gallium nitride (GaN). These materials are ideal candidates for ferrite-semiconductor integration because of their compatibility with high power, high frequency device operation.<sup>2</sup> Furthermore, 6H-SiC has the same hexagonal crystal structure as barium ferrite (BaFe<sub>12</sub>O<sub>19</sub>, BaM) with a lattice mismatch of 4.38% along (0001) plane providing a suitable substrate for the ferrite film.

Our previous attempts at depositing BaM on 6H-SiC by pulsed laser deposition (PLD) showed promising results with evidence of strong crystal texture in the films as well as magnetic anisotropy fields greater than 15 000 Oe.<sup>3</sup> However, the films from these previous studies were unable to obtain microwave losses, as measured by ferromagnetic resonance peak-to-peak derivative linewidths ( $\Delta H$ ), of less than 1000 Oe. In addition to some random orientation in the film seen by x-ray diffraction (XRD), x-ray photoelectron spectroscopy (XPS) revealed evidence of silicon diffusion to the surface.

It is known that lattice mismatch strain impacts both structure and magnetic properties of a BaM film deposited by

PLD.<sup>4</sup> MgO and Pt have been deposited by PLD and used as a buffer layer between Si and PLD-deposited BaM with some improvement in both structure and magnetic properties.<sup>5,6</sup> Although an MgO buffer is expected to reduce the lattice mismatch between the BaM and the SiC from 4.38% to 1.3%, the use of a PLD-grown MgO buffer did not significantly improve the magnetic quality of the films owing to high porosity and less than optimal crystallite orientation. The magnetic properties of the BaM did improve, however, with the introduction of an interwoven MgO/BaM multilayer at the film-substrate interface.<sup>7</sup> This layered MgO/BaM buffer reduced interface diffusion and, consequently, the  $\Delta H$  decreased to less than 500 Oe.<sup>7</sup> Postdeposition heat treatments were found to be ineffective in further reducing the ferromagnetic resonance (FMR) linewidth. The impact of different initial surfaces on BaM morphology and magnetic hysteresis curves was also observed by Capraro *et al.*,<sup>8</sup> comparing PLD-deposited BaM on silicon to sapphire, and in recent work by Heindl *et al.*,<sup>9</sup> comparing bilayers of barium strontium titanate and BaM on MgO and sapphire substrates.

In this letter, we report on the improved magnetic and structural properties of BaM deposited by PLD on an MgO buffer layer grown by molecular beam epitaxy (MBE). This combined use of MBE to provide a high quality buffer layer followed by the growth of a thick film of BaM by PLD is shown to be a simple and effective method to allow integration of BaM with SiC for microwave device applications. The results show high crystal quality epitaxial films without silicon diffusion and with FMR linewidths of less than 100 Oe.

The 6H-SiC (0001) single crystal wafers, acquired from Cree, Inc., were cleaned in a custom-built hydrogen furnace to produce an atomically smooth stepped surface free of oxygen and carbon contamination and polishing scratches.<sup>10</sup> A 10 nm crystalline MgO (111) film was grown by MBE at ~150 °C on the silicon face of 6H-SiC by using a low-

<sup>a)</sup> Author to whom correspondence should be addressed. Tel.: +1617-373-2990. FAX: +1617-373-2209. Electronic mail: kziemer@coe.neu.edu

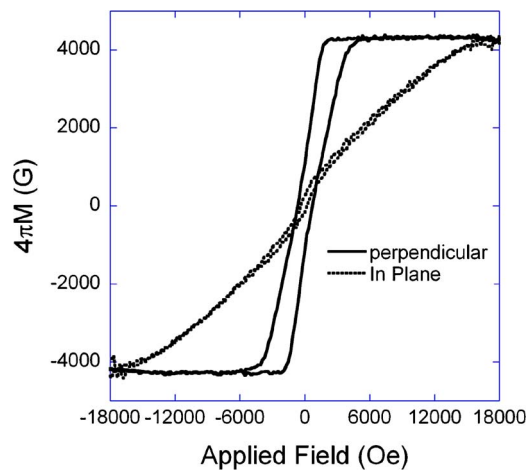


FIG. 1. (Color online) Hysteresis loop obtained by vibrating sample magnetometry with a maximum applied field of 19 000 Oe aligned parallel (dashed) and perpendicular (solid) to the film plane. The sample has been optimally annealed (see text). The perpendicular  $4\pi M_s$  of 4.4 kG compares well to the bulk BaM value of 4.48 kG.

temperature Mg effusion cell and a remote oxygen plasma source. The oxygen plasma was held constant at 100 W and a chamber pressure of  $5 \times 10^{-6}$  Torr. The Mg:O flux ratio was  $\sim 1:20$  which resulted in single crystalline MgO films that grew conformal on the 6H-SiC atomic steps with the epitaxial relationship  $\text{MgO} (111) \parallel 6\text{H-SiC} (0001)$ .<sup>10,11</sup> The MgO buffer layer thickness varied from 2 to 12 nm in this study. Structure and composition of the MgO films were verified *in situ* by reflection high-energy electron diffraction and XPS.

After MBE preparation of the MgO template, the sample was immediately transferred to the PLD chamber. The BaM film was deposited from a homogeneous  $\text{BaFe}_{12}\text{O}_{19}$  target by a Tui KrF excimer laser operating at a wavelength of 248 nm with energy per pulse of 250 mJ. The background gas and substrate temperature were held constant at 20 mTorr pure oxygen and 915 °C, respectively. These conditions were found in previous studies to result in the highest quality BaM films as judged by their magnetic and microwave properties.<sup>3,12</sup> During deposition, in order to promote good adhesion and epitaxy at the interface, the laser repetition rate was slowly raised from 2 to 16 Hz for the first 5 min, and then fixed at 16 Hz for the remaining 30 min of growth.

The dc magnetic properties were measured as room temperature magnetic hysteresis loops via vibrating sample magnetometry (VSM). The applied magnetic field was swept from  $-19$  to  $+19$  kOe with the field aligned both in-plane and out-of-plane sample orientations. Ferromagnetic resonance was measured in the frequency range from 46 to 58 GHz, and the strongest peak-to-peak signal was obtained at 53 GHz. To characterize the crystallographic texture of the BaM film, XRD patterns were obtained from a Bruker D5005 diffractometer and pole figures were obtained using a Philips X'pert thin film diffractometer.

VSM results of the as-deposited BaM on 10 nm of MBE-grown MgO on SiC are shown in Fig. 1. The hysteresis loops confirm that the easy magnetic axis of the BaM film is aligned perpendicular to the film plane. This is consistent with the crystallographic  $c$  axis aligning perpendicular to the sample plane and is the desired orientation for conventional microwave Y-junction circulator device applications. The es-

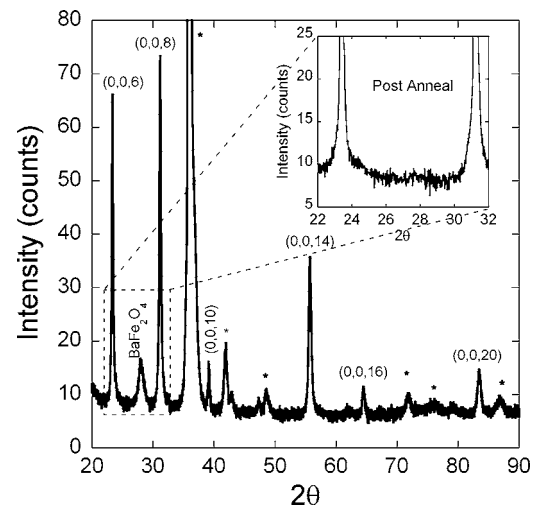


FIG. 2. X-ray diffraction pattern for Ba-hexaferrite ( $M$ -type) film. All significant diffraction features are referenced to  $(0,0,2n)$  indices having a space group of  $P6/mmc$ . The single  $\text{BaFe}_2\text{O}_4$  peak appearing near  $2\theta \sim 27^\circ$  disappeared after a postdeposition annealing procedure (see inset). (\* denotes SiC substrate peaks.)

timated anisotropy field of  $16.9 \pm 0.2$  kOe is in agreement with the published results of the single crystal  $\text{BaFe}_{12}\text{O}_{19}$  value of 17 kOe. In addition, the  $4.4 \pm 0.3$  kG magnetization of the film compares well to the bulk material value of 4.48 kG.<sup>13</sup> XPS depth profile of the as-deposited film showed the bulk of the film contained close to the expected stoichiometric Fe to Ba ratio of 12. No Si diffusion was evident in the BaM film, and no Fe diffusion was evident in the bulk SiC. The abruptness of the BaM/MgO interface suggests very little intermixing at any interface. Atomic force microscopy revealed a smooth surface (1.3 nm root-mean-square roughness over a  $2 \mu\text{m}^2$ ) with indications of layered growth of the as-deposited film.

After deposition, the BaM films were annealed in air at 1050 °C in two steps of 2 min duration each. After annealing, the saturation magnetization increased from 4.3 to 4.4 kG with a  $\Delta H$  of 96 Oe. Figure 2 presents the XRD of the as-deposited film with a segment of the XRD spectrum corresponding to the postannealed film as the inset to the figure. The as-deposited spectrum reveals all  $(0,0,2n)$  diffraction peaks indicating a pure phase magnetoplumbite crystal structure having strong  $c$ -axis orientation perpendicular to the substrate plane. A  $\text{BaFe}_2\text{O}_4$  peak appears near  $2\theta \sim 27^\circ$  signaling the presence of a secondary phase. Evidence for the existence of this phase is eliminated after the annealing procedure.

To fully characterize the texture of the BaM film, pole figures were obtained by tilting the sample and rotating it in a spiral pattern for a fixed value of  $2\theta$ . The angle between the film normal and the line bisecting the incident and detected x-ray beams ( $\phi$ ) was varied from  $0^\circ$  to  $85^\circ$  and the azimuthal angle about the bisecting line ( $\psi$ ) was varied from  $0^\circ$  to  $360^\circ$ . In this work, pole figures were obtained for  $2\theta$  values of  $23.03^\circ$ ,  $17.8^\circ$  and  $30.3^\circ$ , which were chosen to bring the  $\langle 006 \rangle$ ,  $\langle 101 \rangle$ , and  $\langle 110 \rangle$  planes, respectively, into Bragg orientation (JCPDF 84-0757). The pole figure for the  $\langle 006 \rangle$  reflection, which clearly illustrates a single dominant peak and six weaker peaks exhibiting hexagonal symmetry of the as-deposited film, is illustrated in Fig. 3. The center of the pole figure corresponds to the values  $\phi = \psi = 0^\circ$ .  $\phi$  is

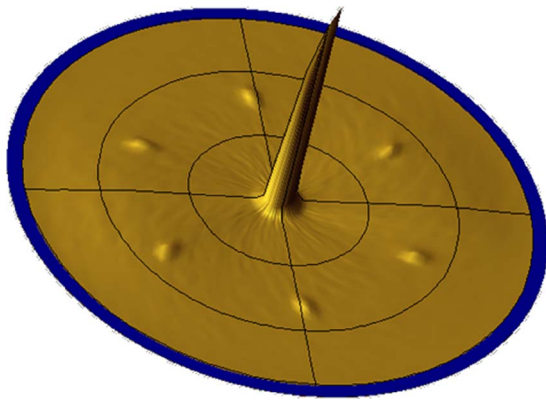


FIG. 3. (Color online) Pole figure obtained for a fixed value of  $2\theta=23.03^\circ$ . The single dominant peak corresponding to  $\phi=\psi=0^\circ$  corresponds to the  $\langle 006 \rangle$  reflection indicating low  $c$ -axis dispersion. The weaker peaks exhibiting sixfold symmetry correspond to the closely spaced  $\langle 104 \rangle$ -type reflections illustrating the epitaxial relationship between the BaM and the MgO buffer layer.

proportional to the radial distance from the center of the pole figure ( $0^\circ < \phi < 90^\circ$ ) and  $\psi$  is the circumferential angle ( $0^\circ < \psi < 360^\circ$ ). The intensity observed in Fig. 3 can be consistently indexed by assuming virtually that all of the grains are oriented with their easy axis within only a few degrees of the sample normal. The single dominant peak about  $\phi=\psi=0^\circ$  corresponds to the  $\langle 006 \rangle$  reflection which is consistent with the  $\theta$ - $2\theta$  data of Fig. 2 and is indicative of low  $c$ -axis dispersion. The six weaker peaks with hexagonal symmetry correspond to the  $\langle 104 \rangle$ -type reflections which exhibit a  $d$  spacing very close to that of the  $\langle 006 \rangle$  peaks ( $2\theta=23.018^\circ$  for  $\langle 006 \rangle$  as compared to  $2\theta=23.225^\circ$  for  $\langle 104 \rangle$ ). The interplanar angle between the  $\langle 104 \rangle$ -type and  $\langle 006 \rangle$ -type planes is  $\sim 48.9^\circ$  as measured from the pole figures. This value agrees well with the expected interplanar angle of  $48.6^\circ$ , which can be estimated using the literature values of the lattice parameters, namely,  $a=0.5892$  nm and  $c=2.3183$  nm.<sup>14</sup> Because the  $\langle 104 \rangle$ -type reflections are observed as well-defined peaks rather than a ring, a strong epitaxial relationship between the BaM and the MgO buffer layer is confirmed.

The FMR linewidth was significantly reduced by the postdeposition heat treatment. The as-deposited films' FMR linewidths of  $\sim 220$  Oe were consistently reduced to  $\sim 100$  Oe after the postdeposition annealing (see Fig. 4), with a consistent 96 Oe after the optimal two-step annealing process described earlier. A  $\Delta H$  value of 96 Oe compares well with values reported for BaM films grown on lattice matched nonsemiconducting substrates, such as MgO and sapphire.<sup>4,15-17</sup> The improvement of the magnetic properties of films after annealing indicates assorted defects within the film have been eliminated by the annealing process. XPS does not show evidence of silicon diffusion at the surface of the annealed films.

In summary, barium hexaferrite films with  $4\pi M_s$  of 4.4 kG and  $\Delta H$  of 220 Oe have been effectively integrated by pulsed laser deposition with single crystal 6H silicon carbide substrates buffered with a 10 nm crystalline MBE-grown MgO (111) layer. The BaM films are characterized as having basal planes parallel to the substrate plane. After an-

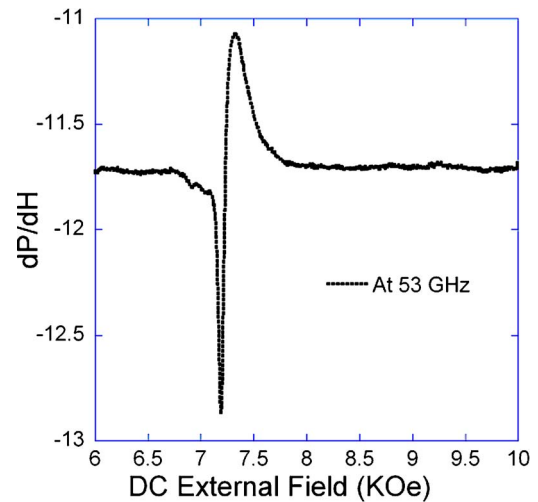


FIG. 4. (Color online) Power derivative as a function of applied magnetic field in the region near the ferromagnetic resonance at 53 GHz. The linewidth measured as the peak-to-peak power derivative is 96 Oe for the post-annealed BaM film deposited on 10 nm MgO (111)||SiC (0001).

nealing, the best films have an FMR derivative power linewidth of 96 Oe, which is of sufficient quality to pursue microwave device applications.

We thank Al Sacco, Jr. at Northeastern University for use of the XRD. This research was supported by the Office of Naval Research (N00014-04-1-0426 and N00014-05-10349) and the Defense Advanced Research Program Agency (HR0011-05-1-0011).

<sup>1</sup>V. G. Harris, Z. Chen, Y. Chen, S. D. Yoon, T. Sakai, A. Gieler, A. Yang, Y. He, K. S. Ziemer, N. Sun, and C. Vittoria, *J. Appl. Phys.* **99**, 08M911 (2006).

<sup>2</sup>I. Zaquine, H. Benazizi, and J. C. Mage, *J. Appl. Phys.* **64**, 5822 (1988).

<sup>3</sup>Z. Chen, A. Yang, S. D. Yoon, K. Ziemer, C. Vittoria, and V. G. Harris, *J. Magn. Magn. Mater.* **301**, 166 (2006).

<sup>4</sup>S. R. Shinde, R. Ramesh, S. E. Lofland, S. M. Bhagat, S. B. Ogale, R. P. Sharma, and T. Venkatesan, *Appl. Phys. Lett.* **72**, 3443 (1998).

<sup>5</sup>X. H. Liu, M. H. Hong, W. D. Song, G. X. Chen, H. M. J. Lam, J. P. Wang, and T. C. Chong, *Appl. Phys. A: Mater. Sci. Process.* **80**, 611 (2005).

<sup>6</sup>X. H. Liu, M. H. Hong, W. D. Song, G. X. Chen, J. P. Wang, Y. H. Wu, and T. C. Chong, *Appl. Phys. A: Mater. Sci. Process.* **78**, 423 (2004).

<sup>7</sup>Z. Chen, A. Yang, Z. Cai, S. D. Yoon, K. Ziemer, C. Vittoria, and V. G. Harris, *IEEE Trans. Magn.* **42**, 2855 (2006).

<sup>8</sup>S. Capraro, J. P. Chatelon, H. Joisten, M. Le Berre, B. Bayard, D. Barbier, and J. J. Rousseau, *J. Appl. Phys.* **93**, 9898 (2003).

<sup>9</sup>R. Heindl, H. Srikanth, S. Witanachchi, P. Mukherjee, A. Heim, G. Matthews, S. Balachandran, S. Natarajan, and T. Weller, *Appl. Phys. Lett.* **90**, 252507 (2007).

<sup>10</sup>T. L. Goodrich, J. Parisi, Z. Cai, and K. S. Ziemer, *Appl. Phys. Lett.* **90**, 042910 (2007).

<sup>11</sup>T. L. Goodrich, Z. Cai, M. D. Losego, J.-P. Maria, and K. S. Ziemer, *J. Vac. Sci. Technol. B* **25**, 1033 (2007).

<sup>12</sup>S. D. Yoon, C. Vittoria, and S. A. Oliver, *J. Appl. Phys.* **92**, 6733 (2002).

<sup>13</sup>Y. Chen, A. L. Geiler, T. Chen, T. Sakai, C. Vittoria, and V. G. Harris, *J. Appl. Phys.* **101**, 09M501 (2007).

<sup>14</sup>Joint Committee Powder Diffraction Files (JCPDF) Card No. 84-0757.

<sup>15</sup>*Magnetic and Other Properties of Oxide and Related Compounds*, Group III: Crystal and Solid State Physics, Vol. 4, edited by K.-H. Hellwege and A. M. Hellwege (Springer, New York, 1970), p. 562.

<sup>16</sup>S. A. Oliver, S. D. Yoon, I. Kozulin, M. L. Chen, and C. Vittoria, *Appl. Phys. Lett.* **76**, 3612 (2000).

<sup>17</sup>Y. Y. Song, S. Kalarickal, and C. E. Patton, *J. Appl. Phys.* **94**, 5103 (2003).